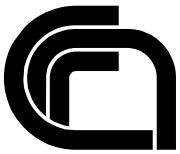

Consiglio Nazionale delle Ricerche

Duty cycling in opportunistic networks: intercontact times and energy-delay tradeoff

E. Biondi, C. Boldrini, A. Passarella, M. Conti

IIT TR-22/2013

Technical report

Dicembre 2013

Istituto di Informatica e Telematica

Duty cycling in opportunistic networks: intercontact times and energy-delay tradeoff

Elisabetta Biondi, Chiara Boldrini, Andrea Passarella, and Marco Conti
IIT-CNR, Via G. Moruzzi 1, 56124 Pisa, Italy
Email: first.last@iit.cnr.it

***Abstract*—Portable mobile devices like smartphones and tablets are the enablers for communications in mobile ad hoc networks. In order to optimise their energy usage, one of the most popular techniques is to implement a duty cycling policy, which periodically puts the user device in a energy saving mode (e.g., Bluetooth *inquiry scan* phase or turning off the WiFi interface) for a certain amount of time. Clearly, this strategy increases the battery lifetime, but it also has the net effect of reducing the number of usable contacts for delivering messages, increasing intercontact times and delays. In order to understand the effect of duty cycling in opportunistic networks, in this paper we propose a general model for deriving the pairwise intercontact times modified by a duty cycling policy. Then, we specialise this model when the original intercontact times are exponential (an assumption popular in the literature), and we show that, in this case, the intercontact times measured after duty cycling are, approximately, again exponential, but with a rate proportional to the inverse of the duty cycle. Once we have the distribution of the intercontact times after duty cycling, we use it for analysing how duty cycling affects the delay of message forwarding and the network lifetime.**

I. Introduction

The widespread availability of smart, handheld devices like smartphones and tablet has stimulated the discussion and research about the possibility of extending the communication opportunities between users. Particularly appealing, towards this direction, is the opportunistic networking paradigm, in which messages arrive to their final destination through consecutive pairwise exchanges between users that are in radio contact with each other. Thus, user mobility, and especially user encounters, are the key enablers of opportunistic communications. This networking paradigm reverses the approach of traditional Mobile Ad Hoc Networks: where user mobility was previously seen as an accident, it is now one of the enablers of message circulation.

One aspect that is hindering opportunistic communications from being widely implemented is the lack of technologies allowing for transparent and efficient ad hoc communications in off-the-shelf smartphones. Severely critical are particularly the energy requirements of such protocols. In fact, it is a well-known problem [1] that WiFi in ad hoc mode is extremely energy hungry, even if idle, and also Bluetooth, generally considered energy-efficient, suffers from high energy consumption during the *inquiry* phase. Clearly, no user will be willing to participate to an opportunistic network if they risk to see their battery drained in a few hours. Due to the energy issues of all the ad hoc communications technologies available, there have been some attempts in the literature to improve the energy efficiency of opportunistic communications. To the best of our knowledge all power saving schemes designed for opportunistic networks focus on contact probing (or, equivalently, neighbour discovery) mechanisms, for two main reasons. First, as discussed in Section II, the neighbour discovery phase is energy hungry for both WiFi and Bluetooth. The second reason is that, in opportunistic networks, nodes are typically not in contact with anyone for a large fraction of time. This implies that, while detecting contacts is crucial and has to be done for the whole network lifetime, continuously scanning without interruptions can be not only energy inefficient but also a waste of time, since often no contact would be detected. Thus, the contact probing phase lends itself to many improvements from the perspective of designing a strategy that misses just a few contacts but provides a high energy gain.

While research on other aspects of opportunistic communications (e.g., routing, data dissemination) has been thriving in the recent years, energy issues in opportunistic networks have still to be fully addressed. Even worse, while there are some works discussing new smart power saving strategies for opportunistic networks, there are very few contributions that study the effect of power saving mechanisms on intercontact times, which are the prominent metric of user contact dynamics and therefore one of the key elements determining forwarding performance. The intercontact time is defined as the time interval between two consecutive encounters between the same pair of nodes. Intercontact times are considered to be the main bottleneck in opportunistic communications, as they are typically one or two orders of magnitude greater than contact times [2]. Being messages exchanged between nodes when they meet, it is clear that the main contribution to message delay is determined by intercontact times. For this reason, we believe it is of paramount importance to understand how power saving techniques, which may effectively reduce the number of usable contacts, affect the intercontact time.

In light of the above discussion, the contribution of this paper is threefold. First, we derive an analytical model of the actual inter-contact times between nodes *after* duty cycling is factored in, i.e. by taking into account that some contacts may be missed because at least one of the devices may be in a low-energy state that does not allow it to detect the contact. In the following, we refer to this figure as *detected* intercontact times. While deriving an exact characterisation of the detected intercontact times is in general too complex from an analytical standpoint, we are able to derive their first two moments. As it is well-known, this is sufficient to approximate the distribution of the detected intercontact times using hyper- or hypo- exponential distributions, using standard techniques [3]. Thus, using this model, we are able to obtain

an approximated representation of intercontact times measured when a duty cycling policy is in place under virtually any distribution.

The second contribution of the paper is the solution of the above model for the case of exponential intercontact times, which is a popular assumption in the related literature [4] [5] (even if a general consensus on which is the best distribution for representing realistic intercontact times has yet to be achieved). With exponential intercontact times, the proposed model can be solved approximately in closed form and, under a specific condition that we derive, the detected intercontact times are still exponential, but with a rate proportional to the inverse of the duty cycle. In addition, we show that the condition under which our approximation holds is satisfied by the most popular traces available in the literature. This result tells us that models (e.g., of the delay) that assume exponential intercontact times (that are typically tractable and thus very popular in the literature) can still be used when a duty cycling policy is in place, as long as the original rates are scaled proportionally to the inverse of the duty cycle. So far, this aspect (i.e., the fact that duty cycling can affect the detected pairwise contacts) has been largely ignored in the literature. In fact, while periodic probing is implemented in almost all contact datasets available in the literature [6] [7] [8], both when studying the statistical properties of intercontact times in the datasets and when using the rates estimated from these traces in order to validate analytical models, the effect of the periodic rather than continuous duty cycling has been ignored.

The third and final contribution of this paper lies in studying how the detected intercontact times affect the delay experienced by messages and network lifetime. As expected, we find that the delay (both first and second moments) increases, but no additional variability is introduced (i.e., the coefficient of variation remains unchanged). Also the network lifetime (i.e., the time until nodes run out of battery, given a certain energy budget) evidently increases. Being the network lifetime longer, a larger volume of traffic is handled by the network when a duty cycling policy is in place. Finally, we focus on the problem of finding an optimal duty cycle value that would allows us to minimise the loss from the delay standpoint and maximise the gain in terms of traffic handled by the network. We show that, when intercontact times are exponential, it is not possible to achieve both goals at the same time and the operator has to decide whether delay or volume of traffic (or equivalently, network lifetime) is of concern.

II. Related work

Ad hoc communications in opportunistic networks typically go through either the WiFi or Bluetooth interface. While for 802.11 cards used in infrastructure mode energy consumption in the idle state (previously comparable to that used in the transmitting/receiving state) has been drastically reduced by the introduction of the Power Saving Mode (PSM) [1], ad hoc 802.11 is still highly inefficient [1] and PSM for ad hoc is typically not implemented in smartphones' 802.11 interfaces. Thus, in the ad hoc case, it is still true that the energy for being idle is comparable to the energy consumed for sending and receiving messages, hence turning off the network cards when possible is the simplest yet the only viable approach for increasing battery lifetime. Measurements of Bluetooth energy consumption are more consistent across past and recent studies. Of all Bluetooth phases, scanning is found to be the most energy hungry across different studies [1], [9]. For this reason, it is often advised to reduce the scanning frequency in order to save battery. The Bluetooth discoverable state is generally considered energy cheap (as stated in [10], [1]) but keeping the phone in the discoverable state indefinitely in the long run incurs in a significant energy consumption as well. In a recent work, Trifunovic et al. [10] directly compare Bluetooth and two innovative WiFi-based ad hoc communications modes, namely, WiFi Direct [11] and WLAN-Opp [12]. As far as neighbor discovery is concerned, Bluetooth is found two times more energy efficient than WLAN-Opp and about five times more energy efficient than WiFi Direct. As expected, the energy consumption for all three protocols heavily depends on the scanning interval, i.e., how often they scan their neighbourhood for new devices. For scanning intervals smaller than $\sim 100s$, the power consumption increases drastically. Looking at energy consumption at a finer detail, we see that, as discussed before, in Bluetooth discovery, the higher amount of energy is consumed during the scanning phase. Instead, for WLAN-Opp both being discoverable (i.e., when the device acts as AP) and discovering are expensive operations. In WiFi Direct the situation is even worse, since for detecting each others both devices have to be scanning at the same time.

A taxonomy proposed by Jun et al. [13] for traditional MANETs classifies duty cycling policies into four categories. With the *synchronous* mechanisms (the most popular of which is 802.11 Power Saving Mode) nodes all wake up/go to sleep at the same time. The drawback of this approach is that it requires a global synchronisation among nodes and a fully connected network[13]. In *asynchronous* strategies, neighbouring nodes select their wake-up slot so that they overlap with one another. In *cell-base* schemes the network is divided into non-overlapping cells, within which only a few nodes are awake at a given time. In *on demand* strategies nodes are equipped with an additional low-power radio interface that is used for signalling wake up or sleep commands. Unfortunately, all the above strategies were designed for a dense and connected network, which is quite different from the typical conditions in which opportunistic networks operate.

As discussed in Section I, all papers dealing with power saving issues in opportunistic networks have focused on the contact probing phase. There are quite a few papers in the literature aiming at designing smart contact probing strategies for DTN/opportunistic networks. Contact probing schemes can be classified into fixed, when the ON/OFF duration of the duty cycle is established at the beginning and never changed [13], or adaptive, when the frequency of probing is increased or decreased according to some policy [14]. Both fixed and adaptive strategies can be context-oblivious [13], if they do not exploit information on user past behaviour or position, or context-aware [15], [16] otherwise. In order to address the lack of duty cycling mechanisms in sparse networks, [13] proposes three schemes based on different availability of information at nodes. In the oracle case, nodes can predict their meetings, so they are able to wake up and get to sleep exactly at the beginning and end of a contact. This strategy is clearly used for benchmarking only, since real nodes are not omniscient. At the opposite range, the authors identify the zero knowledge

strategy, in which nodes have no means to estimate their future contacts, so basically enter a periodic, fixed, beaming period in which neighbour discover is performed. Between these two extremes, the authors propose the partial knowledge strategy, in which they assume that nodes are able to estimate the mean and variance of the intercontact times and the contact times, information that is used in order to predict when to scan more intensely for neighbours (intuitively, not right after a contact has ended).

The work by Choi et al. [14] considers a DTN in which nodes wake up at synchronised intervals and sends beacons in order to discover new neighbours. If no neighbour is discovered, the next beaconing period is set at double the previous interval and nodes sleep until then. This exponential increasing is performed until a maximum value is reached. The main contribution of the paper lies in designing an algorithm (AEB) in order to compute this maximum value in order minimise power consumption and maximise the probability of detecting a contact. This is done exploiting the CDF of contact duration. Unfortunately, this algorithm is targeted at random mobility models (in which contact and intercontact times are i.i.d.), hence it is arguable whether it is applicable to real networks.

An energy-efficient variation of Bluetooth discovery mode is proposed in [15]. This work starts from the observation that wherever a neighbour is encountered, other contacts are likely to happen as well. So the authors propose two schemes: one in which the discovery mode is triggered by indications of recent activities and one in which previous contacts at a specific location (access to a positioning system is assumed) are used to switch the device to a more aggressive scanning mode.

Wang et al. [16], assuming that nodes scan their surroundings every T and that contact duration for a pair of nodes is stationary and i.i.d. are able to prove that among all social-oblivious strategies with the same average contact probing interval, the strategy exploiting fixed probing intervals is optimal for minimising the probability of missing a contact. This is an interesting result, supporting the use of simple fixed contact probing strategies over more elaborate ones. Then, the authors propose some heuristic social-aware adaptive probing algorithm, of which the STAR algorithm, which adapts to the contact arrival process exploiting a self-similar argument, is shown to outperform the others.

The work in [17] is a theoretical work that extends the fluid model of two-hop forwarding with the fact that nodes, with a certain rate, go from the inactive state to the active state (in which they start beaconing until they receive a message copy) and use this model to solve the optimal activation problem. The model is tailored to a homogeneous environment (i.e., nodes with contact process i.i.d.) and, as discussed by the authors themselves, cannot be used as it is to describe the heterogeneous environments seen in real mobility traces. Moreover, the model is not directly applicable to duty-cycling-style power saving, since node activation is considered monotone, i.e., once activated nodes remain active until their battery is depleted or the deadline is reached.

All the above contributions aimed at deriving a power saving strategy for DTNs, be it fixed [13] or adaptive [14], social-oblivious [13] or social-aware [15], [16]. This is not our goal. Instead, in this paper, we assume that a fixed contact probing scheme is given (whether social-oblivious or social-aware is not important, as long as its parameters are kept constant). Our goal is to investigate the effects of such duty cycle in neighbour discovery as far as intercontact times are concerned.

In the literature, the works closest to ours are [18] [19]. Zhou et al. [18] focus on the RWP mobility model and show how the number of contacts detected is affected when neighbour discovery is performed every T seconds and what is the effect on the energy consumption (defined as $1/T$). Our contribution is more general, as it is not bound to the RWP model but it can be applied to any well known distribution for intercontact times, if numerical solutions are sufficient, or it can be solved in closed form for the exponential case. In addition, we also provide an analysis of how the delay is affected by the duty cycling. Moreover, despite its simplicity, our duty cycling function allows for more flexibility than the simple scanning every T seconds, as discussed in the next section.

Qin et al. [19] perform a study that is exactly orthogonal to this work. In fact, they evaluate how link duration (or contact duration, in our terminology) is affected by the contact probing interval. Assuming a fixed, social-oblivious probing scheme similar to the one that we consider, Qin et al. study the effective duration of a contact given that the contact is not discovered immediately when it starts due to the contact probing process in place. They provide a formula for the PDF of the link duration under generic contact duration and study the trade-off between energy (in terms of probing frequency) and throughput. The focus of our work is exactly the opposite. We investigate the effect of contact probing (which can be easily translated into a duty cycling problem) on the intercontact time rather than on the contact time. The motivation for this choice is that intercontact times are typically much larger than contact times in real human mobility, thus the delay in opportunistic networks is mainly determined by the intercontact time. Intercontact times are larger when contacts are not detected immediately or missed and thus it is important to understand how they increase and how this affects the delay experienced by messages.

III. Problem statement

We use duty cycling in a general sense here, meaning any power saving mechanism that hinders the possibility of a continuous scan of the devices in the neighbourhood. So, we assume that nodes can be either in the ON or OFF state. In the ON state, nodes are able to detect contacts with other devices. The semantic of the OFF state depends on the scenario that we want to represent and we will discuss it later in this section. We hereafter focus on a duty cycling technique in which a generic node A is ON for τ_A seconds and OFF for the other $T_A - \tau_A$ seconds, where T_A is the period of the duty cycling scheme. This duty cycling model closely approximates typical duty cycles used in the literature (neglecting the small random back-off time introduced in practice after nodes wake up in order to avoid contention, see e.g., [6]). For example, the proposed duty cycling model is able to model approximately the scanning processes of Bluetooth and WLAN-Opp discussed in [10].

Assuming that the network wakes up at $t = 0$, the first ON interval can be placed anywhere between $[0, T_A)$. We denote with $s_0^{(A)}$ and $s_1^{(A)}$ the time instants at which the ON interval starts and ends, respectively, for which $s_1^{(A)} - s_0^{(A)} = \tau_A$ holds. The duty cycling policy for node A is thus represented by the following function:

$$d_A(t) = \begin{cases} 1 & \text{if } t \bmod T_A \in [s_0^{(A)}, s_1^{(A)}] \\ 0 & \text{otherwise,} \end{cases} \quad (1)$$

where $\bmod$ denotes the modulo operation.

Starting from this duty cycling policy on single nodes, the semantic of the discovery process depends on the specific scenario under study. For example, in the case Bluetooth, assuming that nodes alternate between the *inquiry* and *inquiry scan* phase (corresponding in our model, respectively, to the ON and OFF state) as described in [20], and that ON intervals do not overlap[1], we have that each node is able to detect a contact with nodes in radio range when it is in the ON state. Vice versa, for all scenarios in which for contacts to be detected and used for communications both nodes A and B must be ON at the same time (e.g., as in WiFi Direct), we have to consider the joint duty cycling function[2] d, defined as $d_A * d_B$ (we assume that all nodes have the same period T). The first ON interval of d starts at $s_0 = \max\{s_0^{(A)}, s_0^{(B)}\}$ and ends at $s_1 = \min\{s_1^{(A)}, s_1^{(B)}\}$. We denote the fraction of time nodes spend in the ON period as Δ ($= \frac{\tau}{T}$, where $\tau = s_1 - s_0$ is the length of the ON interval under d and T the period of d).

$$d(t) = \begin{cases} 1 & \text{if } t \bmod T \in [s_0, s_1] \\ 0 & \text{otherwise.} \end{cases} \quad (2)$$

If the ON intervals of nodes A and B never overlap, the two nodes will not be able to communicate, because they never see each other. In order to avoid this trivial case, we assume that duty cycles preserve the ability of nodes to communicate with each other. In the best case, nodes are synchronised, so they are able to fully exploit the length $\min\{\tau_A, \tau_B\}$ of their ON intervals. In the following we will use notation d to generically denote the duty cycling function, be it the single function d_A when only node A needs to be in the ON state for detection or the joint function d.

Function d determines the way contacts are discovered. In the following, we focus on the intercontact process between a generic pair of nodes, and, to make the analysis more tractable, we assume that a contact event is detected only if it starts during an ON period. This assumption is reasonable when the duration of a contact is smaller than the duration of the OFF interval. In fact, in this case the probability of the contact lasting until the next ON interval is negligible. While it is difficult to verify whether this assumption holds for the datasets in which duty cycling is implemented (because the measured contact durations already factor in the duty cycle effect), the work in [2], which relies on special devices with extremely short scanning intervals of $1s$, states that for more than 50% of contact duration samples the duration is smaller than $48s$. Trifunovic et al. [10] have derived that, with Bluetooth and WiFi, scanning intervals greater that $100s$ perform significantly better energy-wise. Actually, typical duty cycling policies used to collect traces have a period of several minutes (e.g., 5 minutes in the Reality Mining dataset [8]), with ON periods in the order of few seconds. Therefore, we can consider this assumption as reasonable.

[1]Please note that with Bluetooth two nodes inquiring at the same time do not detect each other. In a real implementation, overlapping inquiry intervals are avoided by means of the random backoff time.

[2]When unambiguous, we drop the subscript indicating the specific node pair considered, as in this case.

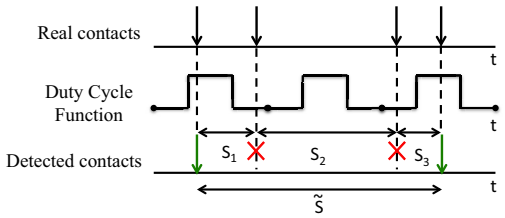

Fig. 1. Contact process with duty cycling

We now focus on the contact process. We assume that the time between two consecutive contacts between the same pair of nodes can be modelled as a continuous random variable S, and that intercontact times between a given pair of nodes are independent and identically distributed (while they can follow different distributions for different pairs). Hence, the contact process can be modelled as a renewal process, where $S_i \sim S$ denotes the time between the i-th and the $(i+1)$ contact event. Similarly, we denote with $\tilde{S}$ the random variable representing the detected intercontact times, and with $\tilde{S}_i \sim \tilde{S}$ the time between the i-th and the $(i+1)$ detected contact event (Figure 1). In the following, without loss of generality, we assume that there is a contact event at t_0 during the first ON period after $t = 0$. Consider the case in which $i-1$ contacts are missed after the one happening at t_0 and the i-th is detected. If we neglect contact duration (recall that this is reasonable, since it is typically one-two orders of magnitude smaller than the intercontact time [6] [2]), it is clear that the time between the two detected events is given by the sum of the interarrival times of the events up to the i-th. Thus, for $\tilde{S}$, the following definition holds.

Definition 1: The detected intercontact time $\tilde{S}$ can be obtained as $\tilde{S} = \sum_{i=1}^{N} S_i$, where N is the random variable describing the number of contacts needed to get one detected.

Therefore, $\tilde{S}$ is a random sum of i.i.d. variables. This sum has some nice properties, which we will exploit in Section V in order to derive the first two moments of $\tilde{S}$. Please also note that Definition 1 is general, i.e., holds for any type of continuous intercontact time distribution and for any type of duty cycling policy. In the next sections we show how the duty cycling model and the contact process can be studied together in order to uncover the features of the detected intercontact times. For the convenience of the reader, the notation used throughout the paper is summarized in Table I.

IV. Deriving the distribution of N

In this section we study the probability distribution of N, defined as the number of contacts needed in order to detect the first one. We aim, in particular, at deriving its first two moments, which are essential, as we will see later in the paper, for the computation of $\tilde{S}$. The rationale behind its derivation is pretty intuitive. In fact, $N = 1$ corresponds to the case of a detection right after the last detected contact. So, if the last

TABLE I. NOTATION

f_X, F_X	PDF and CDF of random variable X
S	intercontact time
$\hat{S}$	detected intercontact time
N	number of ICTs taking places before the next contact is detected
T, τ	period of duty cycle and duration of the ON period
Δ	fraction of time nodes are in ON
t_0	time of the last detected contact
d	duty cycle function
s_0, s_1	start and end time of the first ON period ($s_1 - s_0 = \tau$)
λ_{ij}	rate of intercontact times between nodes i and j
D, D_Δ	delay without duty cycling and delay with duty cycling Δ

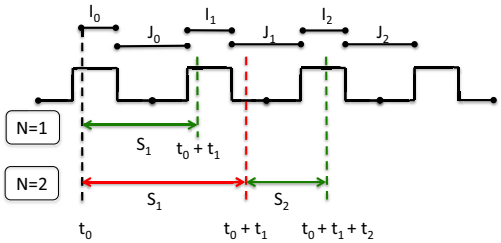

Fig. 2. Example for case $N = 1$ and $N = 2$ (red for missed contact, green for detected contact)

detected contact took place at t_0, with $N = 1$ the next contact can happen in any of the ON intervals after t_0. For case $N = 2$ to happen, the first contact after the one detected at t_0 has to fall in any of the OFF intervals after t_0 ad the second contact in any of the ON intervals after the OFF interval in which the first contact has been missed. The derivation of the PDF of N quantifies the probabilities of each of these events.

Before moving into the detail of the derivation, we first introduce the notation that we use in this section. Let us assume that the last detected contact (we refer to it as the *zero contact*) took place at time t_0. Starting from t_0, we denote the i-th ON interval after t_0 as I_i and the i-th OFF interval after t_0 as J_i. All ON intervals but the first one are of type $[s_0+iT, s_1+iT]$, while all the OFF intervals are defined as $[s_1 + iT, s_0 + (i + 1)T]$. The first ON interval is special, because it is constrained to start after t_0, thus we define it as $(t_0, s1]$. Figure 2 describes this scenario. Then, when N=1, I_{n_1} denotes the ON interval in which the first contact is detected, when N=2 I_{n_2} denotes the ON interval in which the second contact is detected, and so on. We do the same for OFF intervals, thus J_{n_j} denotes the OFF interval in which the j-th contact is missed. We will often use ON and OFF intervals shifted by a time t, which we denote as $I_i - t$ and $J_i - t$. Moreover, we assume that the time t_0 at which the zero contact happens within interval $[s_0, s_1]$ is described by random variable $\hat{S}_0$. Finally, we denote with f_{S_i} the PDF of S_i.

Using the above notation, the PDF of N can be computed as described in Theorem 1 below (the proof can be found in Appendix A). Theorem 1 provides an accurate approximation of the PDF of N when the probability of two undetected contacts falling in the same OFF interval is very low. In Section IV-A we derive the conditions under which this assumption is reasonable and we show that these conditions are satisfied by the most popular traces of human contacts.

Theorem 1 (Distribution of N): The discrete probability density of N can be approximated by the following:

$$P\{N=1\} = \sum_{n_1=0}^{\infty} \int_{s_0}^{s_1} f_{\hat{S}_0}(t_0) \int_{I_{n_1}-t_0} f_{S_1}(t_1) dt_1 dt_0 \quad (3)$$

$$P\{N=2\} = \sum_{n_1=0}^{\infty} \sum_{n_2=n_1+1}^{\infty} \int_{s_0}^{s_1} f_{\hat{S}_0}(t_0) \int_{J_{n_1}-t_0} f_{S_1}(t_1) \cdot \cdot \int_{I_{n_2}-t_0-t_1} f_{S_2}(t_2) dt_0 dt_1 dt_2 \quad (4)$$

$$\vdots$$

$$P\{N=k\} = \sum_{n_1=0}^{\infty} \cdots \sum_{n_k=n_{k-1}+1}^{\infty} \int_{s_0}^{s_1} f_{\hat{S}_0}(t_0) \int_{t_1 \in J_{n_1}-t_0} f_{S_1}(t_1) \cdot \cdots \int_{t_{k-1} \in J_{n_{k-1}}-t_0-\cdots-t_{k-2}} f_{S_{k-1}}(t_{k-1}) \cdot \int_{t_k \in I_{n_k}-t_0-\cdots-t_{k-1}} f_{S_k}(t_k) dt_k dt_{k-1} \ldots dt_1 dt_0. \quad (5)$$

Finding a closed form for the distribution of N in Theorem 1 might be prohibitive in the general case, and we have been able to obtain only numerical solutions. However, when intercontact times are exponential, a closed form solution is available (Corollary 1 below, proof available in Appendix A) and the first two moments of N can be computed (Appendix A).

Corollary 1 (N with exponential intercontact times): When real intercontact times S_i are exponential with rate[3] λ, the probability density of N is given by:

$$\begin{cases} P\{N=1\} = 1 + \frac{e^{-\lambda\tau}-1}{\lambda\tau} + \frac{e^{\lambda\tau}(1-e^{-\lambda\tau})^2}{\lambda\tau(e^{\lambda T}-1)} \\ P\{N=k\} = e^{\lambda\tau} \frac{(1-e^{-\lambda\tau})^2}{\lambda\tau(1-e^{-\lambda T})} \left[\frac{\lambda(T-\tau)}{e^{\lambda T}-1}\right]^{k-1}, \quad k \geq 2 \end{cases} \quad (6)$$

A. Quantifying the error

In Theorem 1 we have provided a general formulation for the distribution of N which holds when the probability of two consecutive contacts happening during the same OFF period is small. We now discuss under which settings the approximation introduced is reasonable, taking as reference the exponential case. Exploiting the result in Corollary 1, it is possibile to compute the error function, as follows.

Definition 2: The error $\mathcal{E}$ (defined in $[0, 1]$) introduced by the approximation in Corollary 1 can be expressed as:

$$\mathcal{E}(\tau, T, \lambda) = \frac{1-e^{-\lambda\tau}}{\lambda\tau} - \frac{e^{\lambda\tau}(1-e^{-\lambda\tau})^2}{\lambda\tau(e^{\lambda T}-1)} + - \frac{e^{\lambda\tau}(1-e^{-\lambda\tau})^2}{1-e^{-\lambda T}} \frac{T-\tau}{\tau(e^{\lambda T}-1-\lambda T+\lambda\tau)}. \quad (7)$$

The above expression can be simply obtained as the difference between 1 and $\sum_k P\{N = k\}$, after noting that in our approximation we are neglecting events that belong to the sample space, hence the total probability that we obtain is

[3]Again, for ease of notation, we omit subscript A, B for λ, since it is unambiguous that we are referring to the tagged node pair A, B. Please note, however, that the network model we are referring to is still heterogenous.

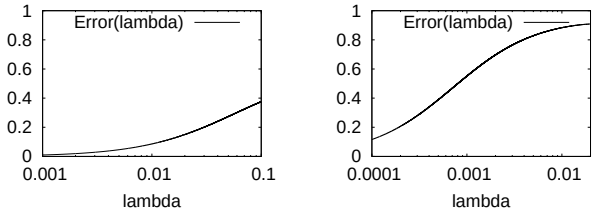

(a) $\tau = 5$ and $T = 15$ (b) $\tau = 5$ and $T = 120$

Fig. 3. $\mathcal{E}$ varying λ (logarithmic scale for the x-axis)

less than 1. The distance between $\sum_k P\{N = k\}$ and 1 thus gives us the quality of our approximation, in which the closer $\mathcal{E}$ to 0 the better.

Intuitively, from a physical standpoint, our approximation holds when the average intercontact time is significantly larger than the duration of the OFF interval. Under this condition, the OFF interval is, on average, too short to accommodate two intercontact times. Thus, the condition when we expect that our approximation is very precise is $E[S] \gg T - \tau$, or, equivalently, $\frac{1}{\lambda} \gg T - \tau$. The worst case for this condition happens when τ is very small. In fact, when $\tau \to 0$ the OFF interval can be as big as possible (i.e., occupying almost all T) and, consequently, the probability that two undetected contacts fall into it maximum. Thus, if we ensure that $\frac{1}{\lambda} \gg T$ our condition will hold. We have proved mathematically this result in Appendix A, which is summarised in the following lemma.

Lemma 1: When $\lambda T \ll 1$, the error $\mathcal{E}$ introduced by the approximation of Corollary 1 approaches zero.

Let us now explore the parameter space τ, T, λ in order to characterise how $\mathcal{E}$ goes to zero when the condition introduced above is satisfied. At first we set $\tau = 5$ and $T = 15$ (as in the RollerNet experiment – see Section V-A) and we plot $\mathcal{E}$ varying λ (Figure 3(a)). As $\frac{1}{\lambda}$ represents the mean intercontact time $E[S]$, the smaller λ the bigger the mean intercontact time. And in fact, the error goes to zero as $\lambda \ll \frac{1}{T-\tau} = \frac{1}{10}$ and our condition is confirmed. We now keep the same τ value and increase T, setting it to $120s$, which is the value used for the Infocom experiment (Section V-A). We expect from condition (i) that the error increases for small λ values with respect to the previous case, and this is confirmed in Figure 3(b).

V. The duty cycling effect on exponential intercontact times

Exploiting the results derived in the previous section, here we discuss how to compute the first and second moment of the detected intercontact time $\tilde{S}$ for a generic node pair A, B. The relation between S and $\tilde{S}$ is stated by Definition 1, i.e., $\tilde{S} = \sum_{i=1}^{N} S_i$. Thus, $\tilde{S}$ is a random sum of random variables, and we can exploit well-known properties to compute compute its first and second moment (in Appendix A we specialise this result for the exponential case).

Proposition 1: The first and second moment of $\tilde{S}$ are given by $E[\tilde{S}] = E[N]E[S]$ and $E[\tilde{S}^2] = E[N^2]E[X]^2 + E[N]E[X^2] - E[N]E[X]^2$.

While the above formula holds in general, in the case of exponential intercontact times it is possible to derive an even stronger result, described in Theorem 2 below. This result is the key derivation of this work, and it tells us that, under condition $\lambda T \ll 1$, exponential intercontact times are modified by duty cycling only in terms of the parameter of their distribution but they still remain exponential.

Theorem 2: When $\lambda T \ll 1$, the detected intercontact times $\tilde{S}$ follow approximately an exponential distribution with rate $\lambda\Delta$.

Proof: We can calculate the moment generating function (MGF) of $\tilde{S}$ using the expression described at the beginning of the section, i.e., $M_{\tilde{S}}(s) = M_N(M_S(s))$. First of all, we have to calculate the MGF of N, that we can obtain from Equation (6). In fact, recalling $\tau = T\Delta$, we have

$$\begin{aligned} M_N(s) &= \sum_{k=0}^{\infty} s^k \cdot P\{N = k\} = \\ &= s\left[1 - \frac{1 - e^{-\lambda T\Delta}}{\lambda T\Delta} + e^{\lambda T\Delta}\frac{(1 - e^{-\lambda T\Delta})^2}{\lambda T\Delta(e^{\lambda T} - 1)}\right] + \\ &\quad + \sum_{k=2}^{\infty} s^k \frac{e^{\lambda T\Delta}(1 - e^{-\lambda T\Delta})^2}{\lambda T\Delta(e^{\lambda T} - 1)}\left[\frac{\lambda T(1-\Delta)}{e^{\lambda T} - 1}\right]^{k-1} \\ &= s\left[1 - \frac{1 - e^{-\lambda T\Delta}}{\lambda T\Delta} + e^{\lambda T\Delta}\frac{(1 - e^{-\lambda T\Delta})^2}{\lambda T\Delta(e^{\lambda T} - 1)}\right] + \\ &\quad + s^2 \frac{e^{\lambda T\Delta}(1 - e^{-\lambda T\Delta})^2}{\Delta(e^{\lambda T} - 1)} \frac{1-\Delta}{e^{\lambda T} - 1 - \lambda T s(1-\Delta)}. \end{aligned}$$

As we are in the hypothesis $\lambda T \ll 1$, we can use the Taylor expansion to find that $M_N(s) = s\Delta + s^2 \frac{\Delta(1-\Delta)}{1-s(1-\Delta)} + \mathrm{o}(1)$. As the MGF of an exponential distribution S is given by $M_S(s) = \frac{\lambda}{\lambda - s}$, we obtain the following:

$$\begin{aligned} M_{\tilde{S}}(s) &= M_N(M_S(s)) = \\ &= \frac{\lambda\Delta}{\lambda - s} + \frac{\lambda^2}{(\lambda - s)^2} \cdot \frac{\Delta(1-\Delta)}{1 - \frac{\lambda}{\lambda - s}(1-\Delta)} + \mathrm{o}(1) = \\ &= \frac{\lambda\Delta}{\lambda\Delta - s} + \mathrm{o}(1). \end{aligned} \tag{8}$$

Since the above equation corresponds, approximately, to the MGF of an exponential random variable with rate $\lambda\Delta$, we conclude that $\tilde{S}$ can be approximated as an exponential random variable with rate $\lambda\Delta$. A longer version of this proof is provided in Appendix A. ■

A. Validation

In this section, we consider the average rate measured in real datasets of human mobility and we verify whether our assumption $\lambda T \ll 1$ is reasonable and whether our model correctly predicts the distributions of the detected intercontact times. For opportunistic networks, there are several publicly available datasets obtained from experiments monitoring contacts between device pairs. Pairwise contacts are typically detected through Bluetooth [6], [7], [8] by means of special devices like iMotes. As we have discussed in Section IV, our model is suitable for this kind of scenarios. Here we consider four popular datasets often used in the related literature: Infocom05 [6], Infocom06 [6], RollerNet [7], and Reality Mining [8]. In Table II we report the average pairwise rate [21] extracted from these traces (corresponding to $\tilde{\lambda}$, i.e., to rates after duty cycling) and the associated λ values obtained applying Theorem 2, under the assumption that ICT are exponential. While this assumption is very strong in general,

TABLE II. QUALITY OF APPROXIMATION IN POPULAR DATASETS

Dataset	T	τ	$\tilde{\lambda}$	λ	λT
Infocom05	120	5	$3.2 \cdot 10^{-4}$	$7.7 \cdot 10^{-3}$	0.92
Infocom06	120	5	$1.13 \cdot 10^{-4}$	$2.7 \cdot 10^{-3}$	0.33
RollerNet	15	5	$4.07 \cdot 10^{-3}$	$1.2 \cdot 10^{-2}$	0.18
Reality	300	5	$1.2 \cdot 10^{-6}$	$7.2 \cdot 10^{-5}$	0.02

Tournoux et al. [7] have shown that it is acceptable for a significant percentage of pairs in some of these datasets. In addition, in Table II we also highlight the duration of the ON period used (corresponding to the duration of the Bluetooth phase in which a device scans for neighbours) and the period of the contact probing process. Using these parameters, we are able to compute λT and check whether our approximation holds (due to space reasons, here we perform an average analysis. A pairwise analysis is provided in Appendix A). As it can be seen in Table II, λT is smaller than 1 in all cases. Clearly, the farther from 1 the better, since we require $\lambda T \ll 1$. Thus, we expect the approximation that we make to be quite good for all datasets except for the Infocom05.

In order to complement the theoretical analysis in Section V, here we verify that our prediction for the distribution of $\tilde{S}$ actually matches simulation results exploiting the parameters of real experiments. Specifically, we take a tagged node pair and we assume that the meeting rate of this pair corresponds to the average meeting rate (average across all pairs of nodes in the traces) measured from the traces in Table II. With this approach we are able to represent the behavior of the average node pair. Then, we draw 10000 samples (100000 for the Reality Mining case, due to the long duty cycle period which led to fewer detections) from an exponential distribution, configured with the parameters λ in Table II. The sequence of these samples corresponds to the contact process between the tagged node pair. To this contact process we apply a duty cycling function with $\Delta = \frac{\tau}{T}$, where τ and T are taken again from Table II. Then we measure $\tilde{S}$ after each detected contact and we plot its CDF for all the four datasets in Figure 4. As expected, for the Infocom06 scenario, there are discrepancies between the actual and predicted values. For the other scenarios, in which the product λT is closer to zero, model prediction are very close to simulation results.

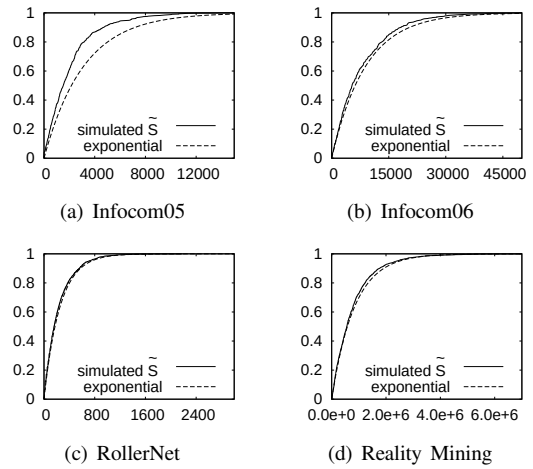

(a) Infocom05 (b) Infocom06

(c) RollerNet (d) Reality Mining

Fig. 4. CDF of $\tilde{S}$ in the different scenarios

VI. THE EFFECT OF DUTY CYCLING ON THE DELAY

In this section we exploit the results on the detected intercontact times derived above in order to compute the first two moments of the delay for a set of representative forwarding strategies designed for opportunistic networks. The first step in this direction is to use the first two moments of the detected pairwise intercontact times for approximating the distribution of the intercontact time itself. Please note that while the analysis in the previous section focused on a tagged pair of nodes, in this section we study the whole network. So, assuming exponential intercontact times, we denote their rates as λ_{ij} for node pair i, j. We have shown that, when assumption $\lambda T \ll 1$ holds, the detected intercontact times follow approximately an exponential distribution. Using this approximation, in the following we solve the analytical model proposed in [22] for both real intercontact times and detected intercontact times. The goal of this evaluation is to study how the first two moments of the delay are affected by energy saving techniques.

The forwarding model that we exploit represents the forwarding process in terms of a Continuous Time Markov Chain (CTMC)[23]. The chain has as many states as the nodes of the network and transitions between states depend both on the meeting process between nodes (i.e., their intercontact times) and on the forwarding protocol in use. Denoting the delay of messages from a generic node i to a tagged node d as D_i, and using standard Markov chain theory, it is possibile to derive the first two moments of D_i as in [22]. We report this result below for the convenience of the reader.

Lemma 2 (Delay's first and second moment): The first and second moment of the delay D_i for a message generated by node i and addressed to node d can be obtained from the minimal non-negative solutions, if they exists, to the following systems, respectively:

$$\forall i \neq d : E[D_i] = \frac{1}{\sum_{j \in \mathcal{R}_i} \lambda_{ij}} + \sum_{j \in \mathcal{R}_s - \{d\}} \frac{\lambda_{ij}}{\sum_{z \in \mathcal{R}_i} \lambda_{iz}} E[D_j] \tag{9}$$

$$\forall i \neq d : E[(D_i)^2] = \frac{2}{[\sum_{j \in \mathcal{R}_i} \lambda_{ij}]^2} + \sum_{j \in \mathcal{R}_s - \{d\}} \frac{\lambda_{ij}}{\sum_{z \in \mathcal{R}_i} \lambda_{iz}} E[D_i^2] + +2 \sum_{j \in \mathcal{R}_s - \{d\}} \frac{\lambda_{ij}}{\sum_{z \in \mathcal{R}_i} \lambda_{iz}} \frac{1}{\sum_{j \in \mathcal{R}_i} \lambda_{ij}} E[D_i] \tag{10}$$

where we denote with $\mathcal{R}_i$ the set of possible relays towards destination d when the message is on node i (this set depends on the forwarding strategy in use). Please note that this model (as most analytical models in the literature) assumes buffers and bandwidth large enough for accommodating all messages.

In [22], we have defined a set of abstract policies able to capture significant aspects of popular state-of-the-art forwarding strategies. In the following we will focus on tthese policies. Under the Direct Transmission (DT) forwarding scheme, the source of the message is only allowed to hand it over to the destination itself, if ever encountered. With the Always Forward (AF) policy, the message is handed over by the

source, and the following relays to the first nodes encountered. Both DT and AF are social-oblivious (also known as context-oblivious or randomized) policies, i.e., they do not exploit information on node social relationships and contact behavior. In [22] two social-aware policies were also defined. In social-aware policies, each intermediate forwarder hands over the message to nodes that have a higher probability of bringing the message closer to the destination, according to some predefined forwarding metrics. The first of these policies is Direct Acquaintance (DA), in which the forwarding metric is the contact rate with the destination ($\frac{1}{E[S_{id}]}$): a better forwarder is one with a higher contact rate with respect to the node currently holding the message. The second policy is Social Forwarding (SF), for which the forwarding metric is $\beta\frac{1}{E[S_{i,d}]} + (1-\beta)\sum_{j\in\mathcal{P}_i} w_{ij}\frac{1}{E[S_{jd}]}$, where $w_{ij} = \frac{\lambda_{ij}}{\sum_{j\in\mathcal{P}_i}\lambda_{ij}}$. With respect to the DA policy, which only captures direct meetings with the destination, SF is also able to detect indirect meetings, allowing nodes to select relays that not only meet the destination frequently but also meet nodes that meet the destination frequently.

In the following we assume that nodes intercontact times are exponential. The fitting analysis presented in [23] has shown that contact rates in the traces already considered in Section V-A follow a Gamma distribution. Below, we focus on the distribution parameters for the RollerNet scenario reported in [21], i.e., shape $\xi = 4.43$, rate $r = 1088$. We consider a network made up of 25 nodes and we solve the forwarding model described above in the case of duty cycle equal to $\frac{5}{15}$, $\frac{10}{15}$ and 1 (no duty cycling). Figures 5-6 show the CDF of the moments of the delay in this case. As expected, both the first and second moment become larger as we reduce the ON interval in the duty cycle. In fact, as discussed before, the neat effect of duty cycling is to effectively reduce the number of usable contacts to only those happening during an ON period. The shorter the ON period, the fewer the usable contacts every T, the longer the delay.

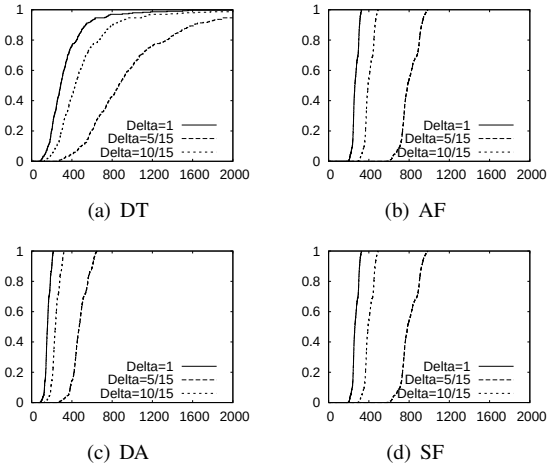

(a) DT (b) AF

(c) DA (d) SF

Fig. 5. CDF of the first moment of the delays for the different forwarding algorithms

Let us now see what happens to the coefficient of variation of the delay (Figure 7). For all pairs, all forwarding strategies and all duty cycling values, the coefficient of variation is bigger than one. This means that the delay can be approximated with

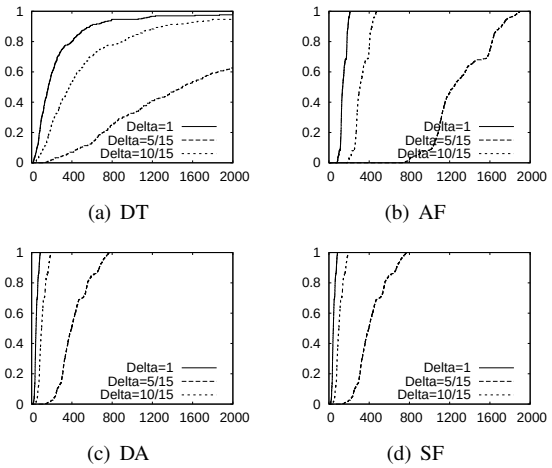

(a) DT (b) AF

(c) DA (d) SF

Fig. 6. CDF of the second moment of the delays for the different forwarding algorithms

an hyper-exponential distribution. In the next section, we will use this representation of the delay in terms of the hyper-exponential distribution in order to compute the volume of traffic carried by the network. Another interesting observation from Figure 7 is that the coefficient of variation does not depend on the duty cycle Δ (in fact, all curves overlap). This means that, in the case of exponential intercontact times, the duty cycle does not introduce variability in the delay experienced by messages.

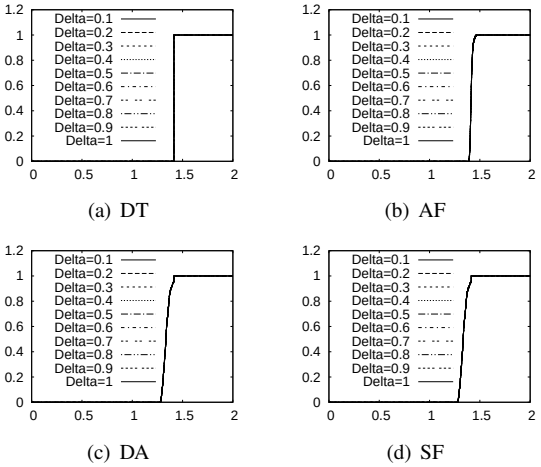

(a) DT (b) AF

(c) DA (d) SF

Fig. 7. CDF of the coefficient of variation of the delay with different Δ

VII. Energy, traffic, and network lifetime

In this section we investigate the benefits of implementing a duty cycling policy on the nodes of the network. These benefits are in terms of energy saved by nodes and, consequently, increased network lifetime. In fact, assuming that nodes have an energy budget L (expressed as the amount of time they can be on when no duty cycling is implemented), by definition nodes' lifetime is extended to $\frac{L}{\Delta}$ when energy saving strategies are in place[4]. At the same time, however, as we have seen in the

[4]We consider only the part of the energy budget related to networking activities.

previous section, the gain in terms of energy is counterbalanced by a loss from the delay standpoint. In fact, the expected delay increases as Δ decreases, so the network lifetime is longer but nodes also need more time to deliver messages.

In the following we want to study the following three aspects. First, what is the relationship between the energy consumed with and without duty cycling. Second, what is the volume of traffic carried by the network with and without duty cycling. Third, whether there exists an optimal duty cycle value for which the loss in terms of delay is minimum and the gain in terms of traffic carried by the network is maximum.

A. Energy with and without duty cycling

We first assume that messages are all generated at time $t = 0$ and that L is very large. The goal here is to understand how much energy is saved by duty cycling, without considering the limited network lifetime, i.e., just taking into account the delivery of standalone messages without temporal limitations. Throughout the section we use a simple energy model in which nodes consume a certain power w (measured in watts) during ON intervals and zero otherwise. In reality, depending on the semantic of the OFF interval, nodes may or may not consume energy. If, for example, the OFF interval corresponds to the *inquiry scan* state of Bluetooth (when the devices listens and responds to inquiries but do not issues inquiries itself) some energy is used (though quite low, see Section II), if it corresponds to devices actually turned off there is instead no consumption. In addition, real devices also consume a significant amount of energy during transmission and reception. Here, however, we have chosen to neglect the consumption due to tx/rx phases for the following reason. Under our approximation, the intercontact rates after duty cycling are equal to the rates before duty cycling scaled by $\frac{1}{\Delta}$. This means that the relative ranking between rates remains the same, and hence the forwarding decisions will remain the same as well. This implies that the number of hops that messages go through with or without duty cycling, in the exponential case, are statistically the same. Since tx/rx energy is associated with each hop, the amount of tx/rx energy consumed with or without duty cycling is the same. Being this amount of energy constant and independent of Δ we have chosen to neglect it and focus instead on the variable consumption.

Below we focus on the expected delay across the whole network, for having a compact representation. Please note however that the behaviour is the same for the single pairs of nodes. We measure the energy consumed as the product between power w and the length of the time interval for which the network is ON. Without duty cycling, the network is ON for the whole time it takes to deliver a message (hence, for $E[D]$), while in case of duty cycling, the network is ON only for a fraction Δ of the time ($E[D_\Delta]$, where we denote with D_Δ the delay under duty cycling Δ) it takes to complete the delivery. In order to measure the relationship between the two quantities, we study the following:

$$R_\Delta = \frac{wE[D]}{w\Delta E[D_\Delta]} = \frac{E[D]}{\Delta E[D_\Delta]}. \tag{11}$$

If the above ratio is around 1, it means that when a duty cycling policy is in place the amount of energy spent is the same but instead of being used all at once it is fractioned and alternated with intervals in which none is used. When the above ratio is greater than 1 we have that the energy required without duty cycling is higher. Vice versa, when the ratio is smaller than 1, the energy needed with duty cycling is higher.

Figure 8 (derived for the same parameters of the RollerNet scenario used above) tells us that the ratio stays around 1 independently of the specific duty cycle value Δ. This result is very interesting, because it shows that under exponential intercontact times the energy consumed for a standalone message is the same, regardless of the value of Δ. With $\Delta = 1$ the energy budget needed for sending the message is simply used all at once, while with $\Delta < 1$ this budget is spread across different intervals of duration T, during which the nodes of network are partially turned off. This is consistent with the assumption of unlimited network lifetime and standalone messages (all generated at $t = 0$) that we have made in this section. In the next section, we discuss instead what happens when nodes have a limited energy budget L and messages are continuously generated by nodes.

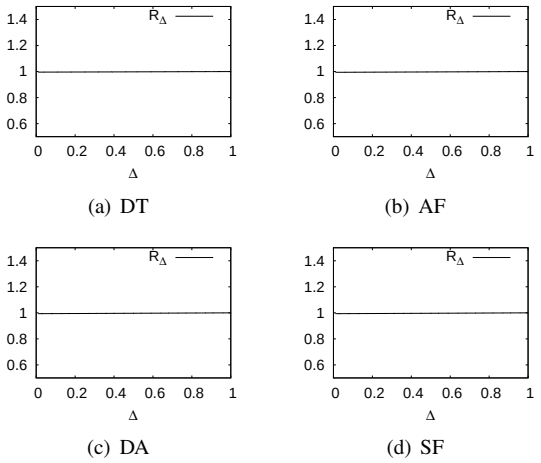

(a) DT (b) AF

(c) DA (d) SF

Fig. 8. R_Δ varying Δ in the different forwarding algorithms

B. Traffic carried by the network

For a more realistic evaluation, we hereafter assume that messages are generated according to a Poisson process with rate μ. By definition, the number of messages created in disjoint timeslots are independent [23]. Thus, the number of messages arriving during a time interval of length dt is given by μdt. When $\Delta = 1$ these messages keep arriving until L, after which the network has exhausted all its energy budget and turns off indefinitely. Instead, when $\Delta < 1$ the network takes longer to consume all its energy budget, thus stays on until $\frac{L}{\Delta}$. In the following we study the volume of messages delivered by the network with and without duty cycling, measured as the number of messages delivered in $\frac{L}{\Delta}$. Then, the following result holds, whose proof can be found in Appendix A.

Theorem 3: The volume N_Δ of messages delivered by the system under duty cycling Δ is given by:

$$N_\Delta = \frac{\mu L}{\Delta} - \mu E[D_\Delta]\left[1 - \frac{1}{2}e^{\frac{-L}{E[D_\Delta]\Delta}}\left(e^{\left(1+\sqrt{\frac{c^2-1}{c^2+1}}\right)} + e^{\left(1-\sqrt{\frac{c^2-1}{c^2+1}}\right)}\right)\right], \tag{12}$$

where c is the coefficient of variation of the delay.

Basically, N_Δ is given by the number of messages generated during the network lifetime (the first term in Equation (12)) minus the number of messages that are not delivered before the energy budget is depleted. The latter quantity is a function of the expected value of the delay and of its variability. We now exploit Theorem 3 in order to study N_Δ. Specifically, in Figure 9 below we show how N_Δ varies with different duty cycles, where we assume that each node generates 1 message every 10 minutes (so $\mu = \frac{1}{600}$). The plot is drawn for a tagged node pair for the sake of readability, but the same results hold for the other pairs. We see that the volume of traffic carried by the network (i.e., the number of messages delivered on average during network lifetime) increases as the duty cycle Δ decreases. So, as expected, increasing the network lifetime more messages get a chance of being delivered but the price to pay, as seen in Section VI, is a larger expected delay.

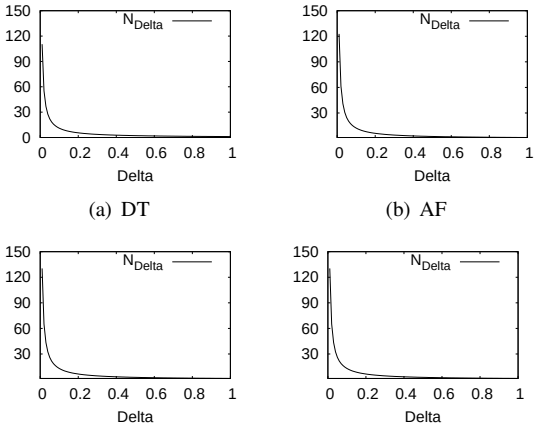

(a) DT (b) AF

(c) DA (d) SF

Fig. 9. N_Δ varying Δ with different forwarding algorithms

C. Trade-off between delay and volume of traffic

In the final part of our evaluation, we study whether it exists an optimal working point that minimises the expected delay and maximises the volume of messages exchanged. We borrow the definition of *power of the network* (which we denote with $\mathcal{W}$) from traditional queueing theory [24]. Quantity $\mathcal{W}$ measures the trade-off between the traffic N_Δ carried by the network (function of the message injection rate μ) and the expected delay $E[D_\Delta]$. The power is then defined as $\mathcal{W} = \frac{N_\Delta}{D_\Delta}$. In traditional queueing systems, the above trade-off was regulated by contention. In fact, under limited resources, we could not increase indefinitely the quantity of messages successfully delivered without affecting the resulting expected delay (because, e.g., under heavy traffic, packets start to be discarded from buffers). In our case, we do not have contention, since we assume that there are no limitations on buffers and bandwidth. Our knob is instead the duty cycle. When Δ approaches 1, delays are as short as possible given the underlying mobility, but a lot of energy is consumed and the network lifetime is shorter. If we want to increase network lifetime, we have to sacrifice the expected delay.

Figure 10 shows how $\mathcal{W}$ varies depending on Δ. It can be clearly seen that $\mathcal{W}$ remains practically constant, which implies that whatever one gains in network lifetime is immediately lost in expected delay. Thus, under exponential intercontact

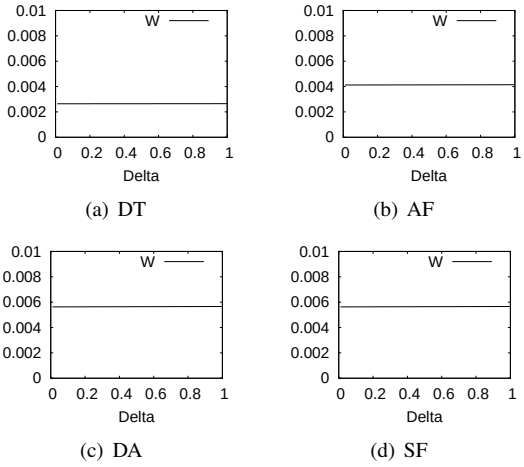

(a) DT (b) AF

(c) DA (d) SF

Fig. 10. $\mathcal{W}$ varying Δ in the different forwarding algorithms ($\mu = \frac{1}{600}$)

times, there is no optimal choice of Δ and all working points are equivalent. When configuring a duty cycling policy, the operator can thus only maximise one metric at a time. Note, anyway, that if the total number of messages to be delivered is of primary concern, at the cost of additional delay, then reducing the duty cycling is clearly effective.

VIII. Conclusion

In this work we have investigated the effects of duty cycling on intercontact times, delay, and energy consumption in opportunistic networks. To the best of our knowledge, this is the first contribution that evaluates the actual effects of duty cycling on the forwarding opportunities between nodes. To this aim, we have provided a general formula for the derivation of the intercontact times under duty cycling, and we have specialised this formula obtaining a closed-form expression for the case of exponential intercontact times. Surprisingly enough, under condition $\lambda T \ll 1$ satisfied by most popular contact datasets, the intercontact times after duty cycling can be approximated as exponentially distributed with a rate scaled by a factor $\frac{1}{\Delta}$. Exploiting this result, we have then studied the first two moments of the delay under duty cycling, showing that these moments both increase as Δ becomes smaller. Finally, we have focused on how the network lifetime is impacted by duty cycling, highlighting the fact that a larger volume of traffic is handled by the network when a duty cycling policy is in place, because the network lifetime is increased even if at the expense of the delay experienced by messages. In addition, we have found that it is not possible to derive an optimal duty cycle value that maximises the network lifetime while at the same time minimally impacting the expected delay.

As future work, two main different directions can be pursued. First, we plan to extend the analysis to intercontact times featuring a distribution different from the exponential, e.g., the Pareto intercontact times case, which also represents a popular hypothesis for the intercontact times considered in the literature [25]. Second, we also plan to evaluate different duty cycling policies, e.g., some in which the duration of ON and OFF intervals is not fixed but varies according to a specified distribution.

ACKNOWLEDGMENT

This work was partially funded by the European Commission under the EINS (FP7-FIRE 288021), MOTO (FP7 317959), and EIT ICT Labs MONC Project (Business Plan 2013) projects.

REFERENCES

[1] R. Friedman, A. Kogan, and Y. Krivolapov, "On power and throughput tradeoffs of wifi and bluetooth in smartphones," *IEEE Trans. on Mob. Comp.*, vol. 12, no. 7, pp. 1363–1376, 2013.

[2] S. Gaito, E. Pagani, and G. P. Rossi, "Strangers help friends to communicate in opportunistic networks," *Computer Networks*, vol. 55, no. 2, pp. 374–385, 2011.

[3] H. Tijms and J. Wiley, *A first course in stochastic models*. Wiley Online Library, 2003, vol. 2.

[4] A. Picu, T. Spyropoulos, and T. Hossmann, "An analysis of the information spreading delay in heterogeneous mobility dtns," in *IEEE WoWMoM*, 2012, pp. 1–10.

[5] W. Gao and G. Cao, "User-centric data dissemination in disruption tolerant networks," in *IEEE INFOCOM*, 2011, pp. 3119–3127.

[6] P. Hui, A. Chaintreau, J. Scott, R. Gass, J. Crowcroft, and C. Diot, "Pocket switched networks and human mobility in conference environments," in *Proceedings of the 2005 ACM SIGCOMM workshop on Delay-tolerant networking*. ACM, 2005, pp. 244–251.

[7] P.-U. Tournoux, J. Leguay, F. Benbadis, J. Whitbeck, V. Conan, and M. D. de Amorim, "Density-aware routing in highly dynamic dtns: The rollernet case," *IEEE Trans. on Mob. Comp.*, vol. 10, no. 12, pp. 1755–1768, 2011.

[8] N. Eagle and A. (Sandy) Pentland, "Reality mining: Sensing complex social systems," *Personal Ubiquitous Comput.*, vol. 10, no. 4, pp. 255–268, 2006.

[9] J.-C. Cano, J.-M. Cano, E. González, C. Calafate, and P. Manzoni, "Power characterization of a bluetooth-based wireless node for ubiquitous computing," in *Wireless and Mobile Communications, 2006. ICWMC'06. International Conference on*. IEEE, 2006, pp. 13–13.

[10] S. Trifunovic, A. Picu, T. Hossmann, and K. A. Hummel, "Slicing the battery pie: fair and efficient energy usage in device-to-device communication via role switching," in *Proceedings of the 8th ACM MobiCom workshop on Challenged networks*. ACM, 2013, pp. 31–36.

[11] "WiFi Direct." [Online]. Available: http://www.wi-fi.org/discover-and-learn/wi-fi-direct

[12] S. Trifunovic, B. Distl, D. Schatzmann, and F. Legendre, "Wifi-opp: ad-hoc-less opportunistic networking," in *Proceedings of the 6th ACM workshop on Challenged networks*. ACM, 2011, pp. 37–42.

[13] H. Jun, M. H. Ammar, and E. W. Zegura, "Power management in delay tolerant networks: a framework and knowledge-based mechanisms." in *IEEE SECON*, vol. 5, 2005, pp. 418–429.

[14] B. J. Choi and X. Shen, "Adaptive exponential beacon period protocol for power saving in delay tolerant networks," in *Communications, 2009. ICC'09. IEEE International Conference on*. IEEE, 2009, pp. 1–6.

[15] C. Drula, C. Amza, F. Rousseau, and A. Duda, "Adaptive energy conserving algorithms for neighbor discovery in opportunistic bluetooth networks," *IEEE JSAC*, vol. 25, no. 1, pp. 96–107, 2007.

[16] W. Wang, M. Motani, and V. Srinivasan, "Opportunistic energy-efficient contact probing in delay-tolerant applications," *IEEE/ACM Transactions on Networking (TON)*, vol. 17, no. 5, pp. 1592–1605, 2009.

[17] E. Altman, A. Azad, T. Başar, and F. De Pellegrini, "Combined optimal control of activation and transmission in delay-tolerant networks," *Networking, IEEE/ACM Transactions on*, vol. 21, no. 2, pp. 482–494, 2013.

[18] H. Zhou, H. Zheng, J. Wu, and J. Chen, "Energy-efficient contact probing in opportunistic mobile networks," in *Proc. of the 22nd International Conference on Computer Communications and Networks*, 2013.

[19] S. Qin, G. Feng, and Y. Zhang, "How the contact-probing mechanism affects the transmission capacity of delay-tolerant networks," *Vehicular Technology, IEEE Transactions on*, vol. 60, no. 4, pp. 1825–1834, 2011.

[20] D. Bohman, M. Frank, P. Martini, and C. Scholz, "Performance of symmetric neighbor discovery in bluetooth ad hoc networks." in *GI Jahrestagung (1)*, 2004, pp. 138–142.

[21] A. Passarella and M. Conti, "Analysis of individual pair and aggregate intercontact times in heterogeneous opportunistic networks," *IEEE Trans. on Mob. Comp.*, vol. 12, no. 12, pp. 2483–2495, 2013.

[22] C. Boldrini, M. Conti, and A. Passarella, "Modelling social-aware forwarding in opportunistic networks," in *Performance Evaluation of Computer and Communication Systems. Milestones and Future Challenges*. Springer, 2011, pp. 141–152.

[23] S. M. Ross, *Introduction to probability models*. Access Online via Elsevier, 2006.

[24] R. Gail and L. Kleinrock, "An invariant property of computer network power," in *Conference Record, International Conference on Communications*, 1981, pp. 63–1.

[25] A. Chaintreau, P. Hui, J. Crowcroft, C. Diot, R. Gass, and J. Scott, "Impact of human mobility on opportunistic forwarding algorithms," *IEEE Trans. on Mob. Comp.*, vol. 6, no. 6, pp. 606–620, 2007.

[26] D. P. Bertsekas and J. N. Tsitsiklis, *Introduction to probability*. Athena Scientific, Belmont, Massachusetts, 2008.

APPENDIX A
PROOFS AND FURTHER RESULTS

Theorem 1 (Distribution of N): The discrete probability density of N can be approximated by the following:

$$P\{N=1\} = \sum_{n_1=0}^{\infty} \int_{s_0}^{s_1} f_{\hat{S}_0}(t_0) \int_{I_{n_1}-t_0} f_{S_1}(t_1) dt_1 dt_0$$

$$P\{N=2\} = \sum_{n_1=0}^{\infty} \sum_{n_2=n_1+1}^{\infty} \int_{s_0}^{s_1} f_{\hat{S}_0}(t_0) \int_{J_{n_1}-t_0} f_{S_1}(t_1) \cdot \cdot \int_{I_{n_2}-t_0-t_1} f_{S_2}(t_2) dt_0 dt_1 dt_2$$

$$\vdots$$

$$P\{N=k\} = \sum_{n_1=0}^{\infty} \cdots \sum_{n_k=n_{k-1}+1}^{\infty} \int_{s_0}^{s_1} f_{\hat{S}_0}(t_0) \int_{t_1 \in J_{n_1}-t_0} f_{S_1}(t_1) \cdot \cdots \int_{t_{k-1} \in J_{n_{k-1}}-t_0-\cdots-t_{k-2}} f_{S_{k-1}}(t_{k-1}) \cdot \int_{t_k \in I_{n_k}-t_0-\cdots-t_{k-1}} f_{S_k}(t_k) dt_k dt_{k-1} \ldots dt_1 dt_0.$$

Proof: Let us start with event $\{N=1\}$. As discussed above, it occurs when the time of the first contact event falls in an ON interval (Figure 2). Recalling that S_1 denotes the interarrival time between the zero and first contact, we require that $t_0 + S_1 \in [t_0, s_1] \cup \bigcup_{n_1=1}^{\infty} I_{n_1}$, i.e, that $t_0 + S_1$ belongs to any of the ON intervals starting from t_0. Forcing a bit the notation in order to have a compact formula, we define $I_0 = (t_0, s_1]$, which corresponds to the usable portion of the first ON interval after t_0. From this consideration we can obtain the following:

$$P\{N=1|\hat{S}_0=t_0\} = \sum_{n_1=0}^{\infty} P(t_0+S_1 \in I_{n_1}) = \sum_{n_1=0}^{\infty} \int_{I_{n_1}-t_0} f_{S_1}(t_1) dt_1.$$

Then, applying the law of total probability, we get $P\{N=1\} = \int_{s_0}^{s_1} P\{N=1|\hat{S}_0=t_0\} * f_{\hat{S}_0}(t_0) dt_0$, from which Equation (3) immediately follows.

Event $\{N = 2\}$ occurs when the first contact happens during an OFF period and the second contact during an ON period (Figure 2). For the first contact to be in an OFF period, we need that $t_0+S_1 \in \bigcup_{n_1=0}^{\infty} J_{n_1}$. For the second contact to be in an ON period we require that $t_0+S_1+S_2 \in \bigcup_{n_2=n_1+1}^{\infty} I_{n_2}$, i.e., that the second contact happens in any of the ON periods *after* the OFF period in which the first contact has been missed. Conditioning on t_0 we can derive $P\{N = 2|\hat{S}_0 = t_0\}$ as follows:

$$P\{N=2|\hat{S}_0=t_0\} = \sum_{n_1=0}^{\infty} P(t_0+S_1 \in J_{n_1}) \cdot$$
$$\cdot P(t_0+S_1+S_2 \in \bigcup_{n_2=n_1+1}^{\infty} I_{n_2} \mid t_0+S_1 \in J_{n_1}) =$$
$$= \sum_{n_1=0}^{\infty} \int_{J_{n_1}-t_0} f_{S_1}(t_1) \sum_{n_2=n_1+1}^{\infty} \int_{I_{n_2}-t_0-t_1} f_{S_2}(t_2) dt_1 dt_2 =$$
$$= \sum_{n_1=0}^{\infty} \sum_{n_2=n_1+1}^{\infty} \int_{J_{n_1}-t_0} f_{S_1}(t_1) \int_{I_{n_2}-t_0-t_1} f_{S_2}(t_2) dt_1 dt_2.$$

Then, if we apply the law of total probability, we get that $P\{N = 2\} = \int_{s_0}^{s_1} P\{N = 2|\hat{S}_0 = t_0\} f_{\hat{S}_0}(t_0) dt_0$, from which Equation (4) follows.

Let us now consider case $\{N = k\}$ with $k \geq 3$, in which there are $k-1$ consecutive failures (i.e., contact events happening during an OFF period) before the first success. Two consecutive undetected contact events can fall in the same OFF interval (i.e., $n_i = n_{i+1}$), or in two different OFF intervals. If we neglect the case of more than one undetected contacts in the same OFF period[5], the complexity of the problem significantly diminish. For this reason, in the following we assume that this is the case in the scenario under study, and in Section IV-A we derive the conditions under which this assumption is reasonable and we show that these conditions are satisfied by the most popular traces of human contacts. So, assuming that the probability that two consecutive missed contacts fall into the same OFF interval is negligible, the probability of event $\{N = k\}$ can be obtained reasoning in the following way:

1) the first contact event (undetected) happens at time $t_0 + S_1 \in J_{n_1}$;
2) assuming $S_1 = t_1$, the second contact event (undetected) happens at time $t_0 + t_1 + S_2 \in J_{n_2}$, with $n_2 > n_1$;

$$\vdots$$

3) assuming $S_{k-2} = t_{k-2}$, the $(k-1)$-th contact event (undetected) happens at time $t_0+t_1+\cdots+t_{k-2}+S_{k-1} \in J_{n_{k-1}}$, with $n_{k-1} > n_{k-2}$;
4) assuming $S_{k-1} = t_{k-1}$, the k-th contact event (detected) happens at time $t_0 + t_1 + \cdots + t_{k-1} + S_k \in I_{n_k}$, with $n_k > n_{k-1}$.

Translating the above into a mathematical formula, following the same line of reasoning used for cases $N = 1$ and $N = 2$, we obtain Equation (5). ■

Corollary 1 (N with exponential intercontact times): When real intercontact times S_i are exponential with rate λ, the probability density of N is given by:

$$\begin{cases} P\{N=1\} = 1 + \frac{e^{-\lambda\tau}-1}{\lambda\tau} + \frac{e^{\lambda\tau}(1-e^{-\lambda\tau})^2}{\lambda\tau(e^{\lambda T}-1} \\ P\{N=k\} = e^{\lambda\tau}\frac{(1-e^{-\lambda\tau})^2}{\lambda\tau(1-e^{-\lambda T})}\left[\frac{\lambda(T-\tau)}{e^{\lambda T}-1}\right]^{k-1}, \quad k \geq 2 \end{cases}$$

Proof: In this proof we show to how solve Theorem 1 when intercontact times feature an exponential distribution. We use the fact that $f_{S_i}(t) = \lambda e^{-\lambda t}$ for the exponential distribution and the following algebraic relation:

$$\sum_{n_1=0}^{\infty} \sum_{n_2=n_1+1}^{\infty} \cdots \sum_{n_{k-1}=n_{k-2}+1}^{\infty} \sum_{n_k=n_{k-1}+1} x^{n_k} = \frac{x^{k-1}}{(1-x)^k}, \tag{A1}$$

that is true for every $|x| < 1$. We omit the proof for $P\{N = 1\}$ and $P\{N = 2\}$ since it is straightforward to solve them once substituting into Equations (3)-(4) $f_{S_i}(t) = \lambda e^{-\lambda t}$ and $f_{\hat{S}_0}(t_0)$ that we discuss below.

So, let us focus on $P\{N = k\}$. $P\{N = k|\hat{S}_0 = t_0\}$ can be obtained from Equation (5) as described below:

$$\begin{aligned} &P\{N=k|\hat{S}_0=t_0\} = \\ &= \sum_{n_1=0}^{\infty} \cdots \sum_{n_k=n_{k-1}+1}^{\infty} \int_{t_1 \in J_{n_1}} \lambda e^{-\lambda(t_1-t_0)} \\ &\quad \int_{t_2 \in J_{n_2}} \lambda e^{-\lambda(t_2-t_1)} \cdots \\ &\quad \cdots \int_{t_{k-1} \in J_{n_{k-1}}} \lambda e^{-\lambda(t_{k-1}-t_{k-2})} \\ &\quad \int_{t_k \in I_{n_k}} \lambda e^{-\lambda(t_k-t_{k-1})} dt_k dt_{k-1} \ldots dt_1 \\ &= \lambda^{k-1}(s_0+T-s_1)^{k-1} e^{\lambda t_0} \left(e^{-\lambda s_0} - e^{-\lambda s_1}\right) \\ &\quad \sum_{n_1=0}^{\infty} \sum_{n_2=n_1+1}^{\infty} \cdots \sum_{n_{k-1}=n_{k-2}+1}^{\infty} \sum_{n_k=n_{k-1}+1}^{\infty} e^{-\lambda n_k T} \\ &= \lambda^{k-1}(T-\tau)^{k-1} e^{\lambda(t_0-s_0)}(1-e^{-\lambda\tau}) \frac{e^{-(k-1)\lambda T}}{(1-e^{-\lambda T})^k} \\ &= e^{\lambda(t_0-s_0)} \frac{1-e^{-\lambda\tau}}{1-e^{-\lambda T}} \left[\frac{\lambda(T-\tau)}{e^{\lambda T}-1}\right]^{k-1}. \end{aligned}$$

In the above derivation we have used Equation (A1) whith $x = e^{-\lambda T}$, which can be applied as $e^{-\lambda T}$ is positive and smaller than 1. In order to derive $P\{N = k\}$ as $\int_{s_0}^{s_1} f_{\hat{S}_0}(t_0) P\{N = k|\hat{S}_0 = t_0\} \mathrm{d}t_0$, we have to determine the distribution of $\hat{S}_0$. Recall that $\hat{S}_0$ describes the arrival time of the zero event in its ON interval $[s_0, s_1]$. Since we are focusing on exponential intercontact times, the contact process is a Poisson process, hence the probability of an arrival in an interval $[s_0, s_1]$ is uniform over the interval. Thus, we can

[5]Please note that this implies that we also neglect multiple contacts detected in the same ON interval.

easily compute $P\{N=k\}$ as follows:

$$P\{N=k\} = \int_{s_0}^{s_1} \frac{1}{s_1-s_0} P\{N=k|\hat{S}_0=t_0\}dt_0 = \\ = \int_{s_0}^{s_1} \frac{1}{s_1-s_0} e^{\lambda(t_0-s_0)} \frac{1-e^{-\lambda\tau}}{1-e^{-\lambda T}} \left[\frac{\lambda(T-\tau)}{e^{\lambda T}-1}\right]^{k-1} dt_0 = \\ = e^{\lambda\tau} \frac{(1-e^{-\lambda\tau})^2}{\lambda\tau(1-e^{-\lambda T})} \left[\frac{\lambda(T-\tau)}{e^{\lambda T}-1}\right]^{k-1}$$

■

Lemma A1 (First two moments of N): When intercontact times are exponential, the first two moments of N are given by the following:

$$E[N] = 1 - \frac{1-e^{-\lambda\tau}}{\lambda\tau} + \frac{e^{\lambda\tau}(1-e^{-\lambda\tau})^2}{\lambda\tau(e^{\lambda T}-1)} + \\ + (T-\tau)e^{\lambda\tau} \frac{(1-e^{-\lambda\tau})^2}{\tau(1-e^{-\lambda T})} \cdot \\ \cdot \frac{-\lambda(T-\tau)+2e^{\lambda T}-2}{(e^{\lambda T}-1-\lambda(T-\tau))^2} \quad \text{(A2)}$$

$$E[N^2] = 1 - \frac{1-e^{-\lambda\tau}}{\lambda\tau} + \frac{e^{\lambda\tau}(1-e^{-\lambda\tau})^2}{\lambda\tau(e^{\lambda T}-1)} + \\ + (T-\tau)e^{\lambda\tau} \frac{(1-e^{-\lambda\tau})^2}{\tau(1-e^{-\lambda T})} \cdot \\ \cdot \frac{\lambda^2(T-\tau)^2 - 3\lambda(T-\tau)(e^{\lambda T}-1)+4(e^{\lambda T}-1)^2}{(e^{\lambda T}-1-\lambda(T-\tau))^3} \quad \text{(A3)}$$

Proof: Using the formula in Equation (6) we can calculate the first and the second moments of N, using the properties of the geometrical series. In fact the first moment can be computed, from standard probability theory, as follows:

$$E[N] = \sum_{k=1}^{\infty} kP\{N=k\} = \\ = 1 - \frac{1-e^{-\lambda\tau}}{\lambda\tau} + \frac{e^{\lambda\tau}(1-e^{-\lambda\tau})^2}{\lambda\tau(e^{\lambda T}-1)} \\ + \sum_{k=2}^{\infty} k \frac{e^{\lambda\tau}(1-e^{-\lambda\tau})^2}{\lambda\tau(1-e^{-\lambda T})} \left[\frac{\lambda(T-\tau)}{e^{\lambda T}-1}\right]^{k-1}.$$

If we are able to show that $\left|\frac{\lambda(T-\tau)}{e^{\lambda T}-1}\right|$ is smaller than 1 we can apply identity $\sum_{k=2}^{\infty} kx^{k-1} = \frac{x(2-x)}{(x-1)^2}$, which holds when $|x|<1$. To this aim, we can rewrite $\frac{\lambda(T-\tau)}{e^{\lambda T}-1}$ as $\frac{\lambda T(1-\Delta)}{e^{\lambda T}-1}$ and observe that this quantity is always greater than or equal to zero. Hence, we can study inequality $\frac{\lambda T(1-\Delta)}{e^{\lambda T}-1} < 1$ and investigate whether it is satisfied or not. The above can be rewritten as $\frac{e^{\lambda T}-1-\lambda T(1-\Delta)}{e^{\lambda T}-1} > 0$. The denominator is by definition greater than or equal to zero, so we can focus on the enumerator. Function $g(y) = e^y - y(1-\Delta) - 1$ is increasing for $y>0$ and such that $g(0)=0$. So $g(y)$ is positive for every positive y, from which follows that identity $\sum_{k=2}^{\infty} kx^{k-1} = \frac{x(2-x)}{(x-1)^2}$ can be applied. After simple mathematical substitutions we then obtain Equation (A2).

The second moment can be obtained as $\sum_{k=1}^{N} k^2 * P\{N=k\}$, from which the equation below follows:

$$E[N^2] = \sum_{k=1}^{\infty} k^2 P\{N=k\} = \\ = 1 - \frac{1-e^{-\lambda\tau}}{\lambda\tau} + \frac{e^{\lambda\tau}(1-e^{-\lambda\tau})^2}{\lambda\tau(e^{\lambda T}-1)} \\ + \sum_{k=2}^{\infty} k^2 \frac{e^{\lambda\tau}(1-e^{-\lambda\tau})^2}{\lambda\tau(1-e^{-\lambda T})} \left[\frac{\lambda(T-\tau)}{e^{\lambda T}-1}\right]^{k-1}$$

We have proved above that $\frac{\lambda(T-\tau)}{e^{\lambda T}-1}$ is positive and less than 1. Exploiting this results, we apply identity $\sum_{k=2}^{\infty} k^2 x^{k-1} = -\frac{x(x^2-3x+4)}{(x-1)^3}$, holding for every $|x|<1$, and we obtain Equation (A3). ■

Lemma A2: The first and second moment of $\tilde{S}$ are given by:

$$E[\tilde{S}] = \frac{1}{\lambda} - \frac{1-e^{-\lambda\tau}}{\lambda^2\tau} + \frac{e^{\lambda\tau}(1-e^{-\lambda\tau})}{\lambda^2\tau(e^{\lambda T}-1)} + \\ + (T-\tau)e^{\lambda\tau} \frac{(1-e^{-\lambda\tau})^2}{\lambda\tau(1-e^{-\lambda T})} \cdot \frac{-\lambda(T-\tau)+2e^{\lambda T}-2}{(e^{\lambda T}-1-\lambda(T-\tau))^2} \quad \text{(A4)}$$

$$E[\tilde{S}^2] = \frac{1}{\lambda^2}\left[2 - \frac{2(1-e^{-\lambda\tau})}{\lambda\tau} + \frac{2e^{\lambda\tau}(1-e^{-\lambda\tau})^2}{\lambda\tau(e^{\lambda T}-1)} + \right. \\ + 2(T-\tau)e^{\lambda\tau} \frac{(1-e^{-\lambda\tau})^2}{\tau(1-e^{-\lambda T})} \cdot \\ \left. \cdot \frac{\lambda(T-\tau)[3+\lambda(T-\tau)-3e^{\lambda T}]+3e^{2\lambda T}-6e^{\lambda T}+3}{(e^{\lambda T}-1-\lambda(T-\tau))^3}\right] \quad \text{(A5)}$$

Proof: Exploiting the properties of the random sum of random variables, it is easy to derive ([26] p. 241) that $E[\tilde{S}] = E[N]E[S]$ and $\sigma^2_{\tilde{S}} = E[N]\sigma^2_S + E[S]^2\sigma^2_N$. For the exponential random variable S of parameter λ the first two moments are given by $E[S] = \frac{1}{\lambda}$ and $E[S^2] = \frac{2}{\lambda^2}$. The moments of N are given by (A2)-(A3). Substituting these results into $E[\tilde{S}] = E[N]E[S]$, $\sigma^2_{\tilde{S}} = E[N]\sigma^2_S + E[S]^2\sigma^2_N$, we obtain Equation (A4). ■

Lemma 1: When $\lambda T \ll 1$, the error $\mathcal{E}$ introduced by the approximation of Corollary 1 approaches zero.

Proof: Assuming that condition $\lambda T \ll 1$ holds true, we can use the Taylor series for the exponential function to obtain the following:

$$\mathcal{E}(\tau,T,\lambda) = \frac{1-e^{-\lambda\tau}}{\lambda\tau} - \frac{e^{\lambda\tau}(1-e^{-\lambda\tau})^2}{\lambda\tau(\lambda T + \mathrm{o}(\lambda T)} + \\ - \frac{e^{\lambda\tau}(1-e^{-\lambda\tau})^2(T-\tau)}{\left[\lambda T - \frac{\lambda^2T^2}{2} + \mathrm{o}(\lambda^2T^2)\right]\tau[\lambda\tau + \frac{\lambda^2T^2}{2} + \mathrm{o}(\lambda^2T^2)]} \\ = \frac{1-e^{-\lambda\tau}}{\lambda\tau} - \frac{e^{\lambda\tau}(1-e^{-\lambda\tau})^2}{\lambda\tau(\lambda T + \mathrm{o}(\lambda T))} + \\ - \frac{e^{\lambda\tau}(1-e^{-\lambda\tau})^2(T-\tau)}{\tau[\lambda^2T\tau - \frac{\lambda^3t^2\tau}{2} + \mathrm{o}(\lambda^2T^2)]}$$

Observing that $\tau = \Delta T$ and again using the Taylor series for the exponential function, we approximate the errors as below:

$$\begin{aligned}\mathcal{E}(\tau,T,\lambda)=&\frac{\lambda T\Delta+\mathrm{o}(T\Delta)}{\lambda T\Delta}+\\&-\frac{(1+\lambda T\Delta+\mathrm{o}(\lambda T))(\lambda T\Delta+\mathrm{o}(\lambda T))^2}{\lambda^2T^2\Delta+\mathrm{o}(\lambda^2T^2)}+\\&-\frac{(1+\lambda T\Delta+\mathrm{o}(\lambda T))(\lambda T\Delta+\mathrm{o}(\lambda T))^2T(1-\Delta)}{T\Delta[\lambda^2T^2+\mathrm{o}(\lambda^2T^2)]}=\\=&1+\frac{\lambda^2T^2\Delta^2-\mathrm{o}(\lambda^2T^2)}{\lambda^2T^2\Delta+\mathrm{o}(\lambda^2T^2)}+\\&-\frac{[\lambda^2T^2\Delta^2+\mathrm{o}(\lambda^2T^2)](1-\Delta)}{\Delta[\lambda^2T^2\Delta+\mathrm{o}(\lambda^2T^2)]}+\\=&1+\Delta-\frac{\Delta^2(1-\Delta)}{\Delta^2}+\mathrm{o}(1).\end{aligned}$$

From the above, we have that the error goes to 0 when λT is much smaller than 1. ∎

Theorem 2: When $\lambda T \ll 1$, the detected intercontact times $\tilde{S}$ follow approximately an exponential distribution with rate $\lambda\Delta$.

Proof: We are going to extend here the proof of Theorem 2 given in the body of the paper, analysing the domains of the MGFs that we previously neglected. In fact, to prove that $\tilde{S}$ can be approximated by an exponential distribution with parameter $\lambda\Delta$, we should demonstrate that for $\lambda\Delta \longrightarrow 0$ both the expressions of the MGFs (i.e. what we proved in the body of the paper) and the domains (i.e what we want to study here) are identical.
Observing the equation of $M_N(s)$ of the proof in the body of the paper, we see that $M_N(s)$ is the result of a power series of functions, and, for this reason, it is defined only in the domain D given by the following:

$$\begin{aligned}D=&\left\{s\in\mathbb{R}:\left|\frac{s\lambda T(1-\Delta)}{e^{\lambda T}-1}\right|<1\right\}=\\=&\left\{s\in\mathbb{R}:|s|<\frac{e^{\lambda T}-1}{\lambda T(1-\Delta)}\right\}.\end{aligned}$$

As $M_{\tilde{S}}(s)=M_N(M_S(s))=M_N\left(\frac{\lambda}{\lambda-s}\right)$, we have that the MGF of $\tilde{S}$ is defined for all $\frac{\lambda}{\lambda-s}\in D$. Observing that $\frac{\lambda}{\lambda-s}$ is a positive number (because $s<\lambda$), $M_{\tilde{S}}$ is defined for all s such that:

$$\frac{\lambda}{\lambda-s}<\frac{e^{\lambda T}-1}{\lambda T(1-\Delta)},\Longleftrightarrow\ s<\lambda-\frac{\lambda^2T(1-\Delta)}{e^{\lambda T}-1}. \quad \text{(A6)}$$

When $\lambda T \ll 1$, the relation (A6) tells us that the domain of $M_{\tilde{S}}$ tends to the domain:

$$\{s\in\mathbb{R}:s<\lambda T\},$$

that is the domain of an exponential random variable with rate $\lambda\Delta$. This completes the proof. ∎

Theorem 3: The volume N_Δ of messages delivered by the system under duty cycling Δ is given by:

$$\begin{aligned}N_\Delta\ =\ &\frac{\mu L}{\Delta}-\mu E[D_\Delta]\cdot\\&\cdot\left[1-\frac{1}{2}e^{\frac{L}{E[D_\Delta]\Delta}}\left(e^{-\left(1+\sqrt{\frac{c^2-1}{c^2+1}}\right)}+e^{-\sqrt{\frac{c^2-1}{c^2+1}}}\right)\right],\end{aligned}$$

where c is the coefficient of variation of the delay.

Proof: Every message generated in the network experience a delay that, as we have already seen, has a coefficient of variation that is bigger than 1. For this reason the delay of every message can be approximated with an hyper-exponential random variable with parameters given by the following:

$$\left\{\begin{array}{l}p_1=\frac{1}{2}\left(1+\sqrt{\frac{c^2-1}{c^2+1}}\right)\\ \lambda_1=\frac{2p_1}{E[D_\Delta]}\end{array}\right.\qquad\left\{\begin{array}{l}p_2=1-p_1\\ \lambda_2=\frac{2p_2}{E[D_\Delta]}\end{array}\right. \quad \text{(A7)}$$

Let us denote with T_g the random variable characterising message generation time. If a message is generated at time $T_g=0$, it is delivered if its delay is less than $\frac{L}{\Delta}$. When the message is generated at the time $T_g=t>0$, it arrives at the destination if the delay is less than the remaining time $\frac{L}{\Delta}-t$. For this reason its probability to be delivered is given by

$$\begin{aligned}P\left\{T_g+D_\Delta\leq\frac{L}{\Delta}\middle|T_g=t\right\}=&\\=1-\left(p_1e^{-\lambda_1(\frac{L}{\Delta}-t)}+p_2e^{-\lambda_2(\frac{L}{\Delta}-t)}\right),&\end{aligned}$$

exploiting the CCDF of the hyper-exponential distribution. As in a Poisson process of rate μ, in a time interval dt are generated μdt messages, the total number of messages delivered in the network lifetime $\frac{L}{\Delta}$ is given by:

$$\begin{aligned}N_\Delta=&\int_0^{\frac{L}{\Delta}}P\left\{T_g+D_\Delta\leq\frac{L}{\Delta}\middle|T_g=t\right\}\mu\,dt\\=&\int_0^{\frac{L}{\Delta}}\mu\left[1-\left(p_1e^{-\lambda_1(\frac{L}{\Delta}-t)}+p_2e^{-\lambda_2(\frac{L}{\Delta}-t)}\right)\right]dt\\=&\frac{\mu L}{\Delta}-\mu\left[\frac{p_1}{\lambda_1}\left(1-e^{-\lambda_1\frac{L}{\Delta}}\right)+\frac{p_2}{\lambda_2}\left(1-e^{-\lambda_2\frac{L}{\Delta}}\right)\right]\\=&\frac{\mu L}{\Delta}-\mu\left[E[D_\Delta]-\frac{E[D_\Delta]}{2}\left(e^{-\lambda_1\frac{L}{\Delta}}+e^{-\lambda_2\frac{L}{\Delta}}\right)\right],\end{aligned} \quad \text{(A8)}$$

where we used that $\frac{p_1}{\lambda_1}=\frac{p_2}{\lambda_2}=\frac{E[D_\Delta]}{2}$ from Equation (A7). This concludes the proof. ∎

A. Validation: pairwise analysis

In this section we discuss whether the condition $\lambda T \ll 1$ at the basis of our approximation holds true for the pairs of nodes in the datasets that we have studied in Section V-A, where, due to lack of space, we have only performed an average study. In Figure 11 we have plotted the CDF of quantity λT across all pairs in the datasets. Please note that we have only considered contacts between internal devices (i.e., only those that were explicitly taking part to the experiments). For the Reality Mining datasets, we have neglected contacts during the summer break, as done in previous studies [21]. From Figure 11, it is clear that the results that we have obtained for the average case are able to accurately represent what happens at the level of individual pairs. For the RollerNet and Reality Mining experiments, the vast majority ($> 90\%$) of pairs satisfy the condition for the approximation. In Infocom06 there is still a large fraction of pairs satisfying the approximation, while for Infocom05 the approximation seems to hold for $\sim 60\%-70\%$ of pairs. These pairwise results confirm what we have derived in Section V-A.

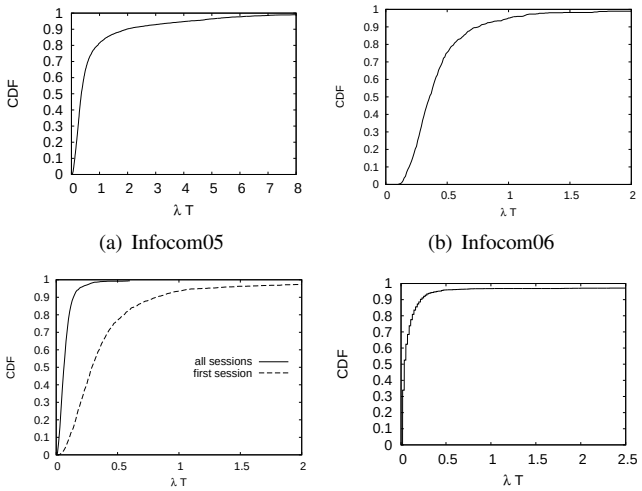

(a) Infocom05 (b) Infocom06

(c) RollerNet (d) Reality Mining

Fig. 11. CDF of λT in the reference datasets